EBioMedicine 61 (2020) 103039

Contents lists available at ScienceDirect

EBioMedicine

journal homepage: www.elsevier.com/locate/ebiom

Research paper

Pharmacological validation of targets regulating CD14 during macrophage differentiation

Gisela Jimenez-Duran[a,f,1], Rosario Luque-Martin[e,1], Meghana Patel[a,i], Emma Koppe[a], Sharon Bernard[b], Catriona Sharp[b], Natalie Buchan[h], Ceara Rea[g], Menno P.J. de Winther[e], Nil Turan[b], Davina Angell[b], Christine A. Wells[k], Rick Cousins[a,j], Palwinder K. Mander[b,1,*], Seth L. Masters[a,c,d,1,*]

[a] Immunology Catalyst, Immunology Network, Adaptive Immunity Research Unit, GSK, Stevenage, UK
[b] Immuno-Epigenetics, Adaptive Immunity Research Unit, GSK, Stevenage, UK
[c] Inflammation Division, The Walter and Eliza Hall Institute of Medical Research, Parkville, Australia
[d] Department of Medical Biology, The University of Melbourne, Parkville, Australia
[e] Department of Medical Biochemistry, Experimental Vascular Biology, Amsterdam Cardiovascular Sciences, Amsterdam UMC, University of Amsterdam, Amsterdam, the Netherlands
[f] Institute of Infection and Immunity, Medical School, University Hospital of Wales, Cardiff University, Wales, UK
[g] Molecular Design, Data and Computational Sciences, GSK, Stevenage, UK
[h] Human Genetics Computational Biology, Human Genetics, GSK, Stevenage, UK
[i] Cambridge Academy of Therapeutic Sciences (CATS), University of Cambridge, 17 Mill Lane, Cambridge, CB2 1RX
[j] Cinnabar Consulting Limited, Bedford, UK
[k] Centre for Stem Cell Systems, Faculty of Medicine, Dentistry and Health Sciences, University of Melbourne, Parkville, Australia

ARTICLE INFO

Article History:
Received 25 June 2020
Revised 13 September 2020
Accepted 14 September 2020
Available online xxx

ABSTRACT

The signalling receptor for LPS, CD14, is a key marker of, and facilitator for, pro-inflammatory macrophage function. Pro-inflammatory macrophage differentiation remains a process facilitating a broad array of disease pathologies, and has recently emerged as a potential target against cytokine storm in COVID19. Here, we perform a whole-genome CRISPR screen to identify essential nodes regulating CD14 expression in myeloid cells, using the differentiation of THP-1 cells as a starting point. This strategy uncovers many known pathways required for CD14 expression and regulating macrophage differentiation while additionally providing a list of novel targets either promoting or limiting this process. To speed translation of these results, we have then taken the approach of independently validating hits from the screen using well-curated small molecules. In this manner, we identify pharmacologically tractable hits that can either increase CD14 expression on non-differentiated monocytes or prevent CD14 upregulation during macrophage differentiation. An inhibitor for one of these targets, MAP2K3, translates through to studies on primary human monocytes, where it prevents upregulation of CD14 following M-CSF induced differentiation, and pro-inflammatory cytokine production in response to LPS. Therefore, this screening cascade has rapidly identified pharmacologically tractable nodes regulating a critical disease-relevant process.

Introduction

Macrophages are key players in tissue homeostasis and inflammation but can also contribute to a diverse range of human diseases, including inflammatory, metabolic, and cardiovascular diseases [1,2]. Circulating monocytes can infiltrate inflamed tissues where they differentiate into monocyte-derived macrophages (MDM). Cluster of differentiation 14 (CD14) was described as a monocyte/macrophage differentiation antigen on the surface of myeloid lineages, such as monocytes, macrophages and dendritic cells (DCs) [3]. In humans, circulating monocytes generated in the bone marrow have been separated into different subtypes. The first, defined as "classical monocytes" (approximately 85%) express CD14 but are negative for CD16 ($CD14^{+ve}CD16^{-ve}$). The second subset are termed "non-classical monocytes", represent 5–10% of total monocytes, which are defined as $CD14^{low}CD16^{+ve}$ [4]. The third subset termed "intermediate"

* Corresponding authors.
E-mail addresses: palwinder.k.mander@gsk.com (P.K. Mander), masters@wehi.edu.au (S.L. Masters).
[1] Equal authorship contribution

https://doi.org/10.1016/j.ebiom.2020.103039

Research in context

Evidence before this study

CD14 is a co-receptor for bacterial LPS, and can potentiate inflammatory signalling when upregulated on myeloid cells during differentiation. To date, the genetic control of CD14 upregulation during this process remains poorly studied. Therefore, we performed a CRISPR screen in monocytic Thp1 cells, differentiated into macrophages using PMA, using CD14 as a readout.

Added value of this study

To rapidly translate the hits from our screen, they were validated using small molecule inhibitors in both cellular and functional assays. This identifies one inhibitor, iMAP2K3, which prevents upregulation of CD14 on primary human monocytes differentiated with M-CSF, and subsequent pro-inflammatory cytokine production in response to LPS.

Implications of this study

This genetic screen identifies a number of novel targets regulating CD14 expression by macrophages. These cells are implicated in a broad array of disease pathologies, and CD14 has recently been associated with cytokine storm in COVID19. Therefore, targeting MAP2K3 could be an important anti-inflammatory therapy.

($CD14^{+ve}$ $CD16^{+ve}$), is currently under debate regarding whether these cells are different, or just in transition between the classical and non-classical subtypes [5,6]. "Classical" monocytes tend to be recruited into tissues first and at higher levels under inflammatory conditions, whilst "non-classical" have a patrolling function [7–10]. However the precise role of different monocyte subtypes is still far from clear [11].

CD14 plays a crucial role in the phagocytic clearance of apoptotic cells and in the reactivation and immune recognition of microbial cell wall components from Gram-positive and Gram-negative bacteria [12]. Furthermore, CD14 is widely reported to associate with the toll-like receptor 4 (TLR4) by binding to LPS and eliciting a cascade of inflammatory signaling [13] and TLR4 endocytosis [14]. CD14 exists in two forms, a 52-55 kDa protein, mCD14, attached to the membrane by a glycosylphosphatidylinositol (GPI) anchor, and the serum soluble 48–56 kDa sCD14, an acute-phase protein [15]. In this way, sCD14 can potentiate LPS transfer to trigger TLR4 on cells that do not express mCD14 [16–18]. The physiological relevance of CD14 was confirmed in knockout mice which do not respond to low dose LPS in the production of TNF, IL-1β and IP-10 [19], however ingestion of sCD14 restores their capacity to mount this inflammatory response [20].

In pathogenesis where monocytes infiltrate peripheral tissues and differentiate into macrophages, CD14 expression has been markedly upregulated and may contribute to, or aid resolution of disease, depending on context [21]. Therefore, inhibitors that prevent upregulation of CD14 may find utility in a variety of inflammatory diseases, but increasing CD14 expression could also potentiate anti-tumor or vaccine responses. Most recently, Martin and colleagues have proposed CD14 as a target to treat cytokine storm in COVID19 [22]. The foundation for this is the observation that the plasma concentration of soluble CD14 (sCD14) is increased in severely affected patients [23]. Moreover, patients with Acute Respiratory Distress Syndrome (ARDS) have elevated levels of sCD14 in bronchoalveolar lavage (BAL) fluid [24], and there was a small clinical trial (7 treated, 6 controls) of a neutralizing antibody against CD14 which demonstrated a trend towards reduced neutrophils and cytokine concentrations in BAL fluid (Implicit Bioscience Ltd., data on file for IND12209).

In this study, we wanted to identify regulators of macrophage differentiation and CD14 in human macrophages. To accomplish that, we used Clustered Regularly Interspaced Short Palindromic Repeats (CRISPR) with pooled sgRNA screening technology, which allows simultaneous knockout of thousands of individual genes. Here, a whole-genome CRISPR/ Cas9 screen was performed in human THP-1 cells to understand which genes regulate the differentiation of inflammatory macrophages, based on changes in CD14 expression. We identified genes that downregulated CD14 after differentiation of THP-1 cells with PMA and others that promoted differentiation by increasing CD14 expression in cells not treated with PMA. Given the pressing need for drugs that might reduce CD14 to treat cytokine storm in COVID19 patients, we wanted to translate the screen hits as quickly as possible. To this end, we performed validation using existing pharmacological inhibitors, revealing a molecule targeting MAP2K3 which can prevent CD14 upregulation on primary human M-CSF derived macrophages.

Methods

Culture, differentiation and treatment of THP-1 cells

THP-1 cells (ATCC® TIB202™) were cultured using RPMI-1640 (Life Technologies) supplemented with 2 mM L-glutamine, 10% FCS and Penstrep (100 U/ml) at 37°C, 5% CO_2. Cells were grown to a density of 5×10^5–1×10^6 cells/ml and used for experiments between passage 5 and 12. For THP-1 compound treatment and differentiation, cells were seeded in plates and incubated with the corresponding GSK compounds (Supplementary table 1) or 0.1% DMSO in the controls for 30 min. Cells were then left untreated or treated with Phorbol-12-myristate 13-acetate (PMA) (100 ng/ml) (Sigma-Aldrich) for 48 h at 37°C, 5% CO_2 to allow differentiation. After 48 h, cells were analysed by flow cytometry.

Primary monocyte differentiation and treatment

Human PBMCs were isolated from whole blood from healthy donors by gradient centrifugation. Monocytes were purified from PBMCs using CD14+ beads (Miltenyi Biotech) according to supplier's protocol. Purified monocytes treated with growth factor M-CSF (100 ng/ml) (R&D Systems) were cultured in RPMI-1640 (Life Technologies) with 2 mM L-glutamine, 5% FCS and PenStrep (100 U/ml). Blood monocytes were treated with the corresponding GSK compounds (Supplementary Table 1) or 0.1% DMSO for 5 days at 37°C, 5% CO2 to allow differentiation. On day 5, cells were analysed by flow cytometry or stimulated with LPS (100 ng/ml; Sigma L4391) for 24 h, from which supernatants were collected for cytokine analysis. All human biological samples were sourced ethically, and their research use was in accord with the terms of the informed consents under an IRB/EC approved protocol.

Cytokine assays

Supernatants were collected and IL-1β, IL-6 and TNF were quantified by Human Pro-Inflammatory 7-Plex Tissue Culture Kit (Mesoscale) in accordance with the supplier's protocol.

Concentration-response study

THP-1 cells were differentiated in the presence of PMA (100 ng/ml) for 48 h in combination with increasing concentrations of the

different compounds tested (10 μM, 3.3 μM, 1.1 μM, 370 nM, 123 nM, 41.1 nM, 13.7 nM, 4.5 nM 0 nM). After 48 h the viability was determined based on the ATP levels of the cells using CellTiter-Glo kit following manufacturer's instructions. Viability is represented in percentage after normalization of the ATP values to the PMA condition without compound. MMP-9 production was measured in the supernatants using MSD MMP-9 kit (Mesoscale) according to supplier's instructions. Data is represented in percentage of response in a non-linear curve for concentration-response data.

Flow cytometry

MDMs and THP-1 cells were detached using a Cell Dissociation buffer (Sigma-Aldrich), followed by 2 washes in PBS and stained with Live/dead stain (Annexin V) (BD Biosciences, #565388) for 15 min at room temperature. Cells were washed twice with FACS buffer (BioLegend) and incubated with an Fc receptor blocking agent (Human TruStain FcX, BioLegend #422302) for 10 min at room temperature, prior to incubation with CD14 antibody (Biolegend, #325604) for 30 min at room temperature. Flow cytometric analysis was performed on a BD FACSCanto II flow cytometer.

Genome wide CRISPR Cas9 screening in THP-1 cells

CRISPR screens were conducted at Horizon Discovery (Cambridge, UK).

Library generation

A whole genome library was developed that exploited informatically optimised guides (25) expressed in tandem with a modified tracrRNA sequence (5'-GTTTAAGAGCTATGCTGGAAACAGCATAGCAA GTT-3') (26) was used. An all-in-one lentivirus plasmid vector was built comprising a selection marker (puromycin resistance), the expression cassette for Cas9 and the sgRNA sequence and cloned by Gibson Assembly (New England BioLabs, NEB #E2611S/L) in accordance with the manufacturer's instructions. Library plasmids were purified using a Qiagen Plasmid Plus purification system in accordance with the manufacturer's instructions.

Lentivirus production

HEK293T cells (ATCC, USA) were grown in DMEM and 10% FBS (Gibco, UK) and transfected with the library plasmids using Lipofectamine 3000 (Invitrogen, USA) and Virapower packaging virus (Life-Technologies, UK) in accordance with the manufacturer's instructions. After 48 h the medium was removed and centrifuged at 500 x g for 10 min at 4°C. The virus was further concentrated using Lenti-X concentrator (Clontech #631232) in accordance with the manufacturer's instructions. The viral supernatant was aliquoted and stored at -80 ^{0}C in DMEM with 10% FBS and 1% BSA.

Cell transduction, staining and screening protocol

Cells were trypsinized, seeded in complete medium supplemented with 8 μg/ml polybrene (Sigma-Aldrich) and seeded into 12 well dishes at 2×10^6 cells per well and spinfected for 2 h at 2000 rpm at 37 ^{0}C using virus diluted to achieve a MOI of 0.3. At least 1×10^8 of THP-1 cells were transduced, resuspended, transferred to a 50 ml falcon and centrifuged at 1000 rpm for 5 min. The supernatant was removed, and cells were resuspended in 50 ml fresh media (without polybrene) and after 48 h cells were treated with puromycin at a final concentration of 1 μg/ml. PMA treatment occurred 18 days after transduction (11 days of puromycin selection followed by 7 days of expansion).

Following the completion of antibiotic selection, cells were separated into replicates and treatment groups (DMSO-treated THP-1 monocytes, PMA-treated adherent and suspension macrophages), of at least 3.6×10^7 cell per condition and grown in continuous culture to enact editing. For staining, cells were diluted to 2×10^6 cells/ml in FACS buffer (PBS, 2% FBS, 2 mM EDTA). Cells were incubated with an Fc receptor blocking agent (Human TruStain FcX, BioLegend 422302, 1:100) for 10 min at room temperature prior to incubation with primary CD14 antibody (CD14-AF488 HCD14 IgG1, BioLegend 325610, 5 μl/2 $\times 10^6$ cells) for 45 min at 4°C, followed by 2 washes in PBS. Non-viable cells were stained with a fixable viability dye ZombieNIR (BioLegend 423105, 1:500) for 30 min at room temperature, followed by 2 washes in FACS buffer. Finally, cells were fixed with 4% PFA (BioLegend 420801) for 20 min at room temperature, followed by 2 washes in FACS buffer. All 3 treatment groups were analysed by flow cytometry. DMSO-treated monocytes (stained with isotype control and CD14 antibody) were used to determine the $CD14^{-ve}$ gate. Subsequently, the $CD14^{+ve}$ gate was drawn next to the negative gate, and all screen samples sorted based on CD14 negative and positive gates, so CD14 positive cells were separated from CD14 negative cells. Cell pellets were collected and stored at -80°C. All samples were then thawed and gDNA extracted using Qiagen Blood Maxi kit. DNA concentration was determined using a Nanodrop spectrophotometer and at least 230 μg of genomic DNA for each sample was then amplified with PCR to generate amplicons of the sgRNA cassette using a forward primer:

TCGTCGGCAGCGTCAGATGTGTATAAGAGACAGU−[Variable]−TGTGGAAAGGACGAAACACC;

and a reverse primer:

GTCTCGTGGGCTCGGAGATGTGTATAAGAGACAGGATCAATTGCC-GACCCCTCC. These amplicon samples were purified using Agencourt beads (Beckman) and deep sequenced on an Illumina NextSeq platform/system (Microsynth AG, Switzerland).

Data analysis

Statistical analysis

Data represent the mean ± standard error of the mean (SEM). Differences between groups are analysed using an unpaired student's *t*-test using Prism 7 (GraphPad software, La Jolla, California). Differences were considered significant when the *p* value was $\leq$ 0.05 (*), 0.01 (**), 0.001 (***), 0.0001 (****).

Flow cytometry

FSC files were exported and analysed in FlowJo software version 10.4.2. For the gating strategy doublets were removed and then live cells were selected. From live cells, $CD14^{+ve}$ cells were gated based on CD14 FMO and the percentage and MFI of CD14 positive cells was measured and exported.

CRISPR screen

Conducted at Horizon Discovery (Cambridge, UK). Raw NGS libraries were evaluated for quality using FASTQC version 0.11.5. (Babraham Institute, Cambridge UK). Guide counts were obtained using an in-house customized version of the MAGeCK workflow version 0.5.56, which took into account guide staggering from the experimental protocol. Briefly, guides were trimmed and mapped with exact string counts from each file to provide raw counts for each guide found in the library. Guide counts were normalised within each group (median-based) and Log2 fold change (LogFC) was calculated to determine the change in abundance of each guide in each sample. RRA values (p-values) were determined using the MAGeCK algorithm (version 0.5.56), as described in Li et al (27). Specific comparison data was extracted and used for volcano plot generation in TIBCO Spotfire v7.11.1.

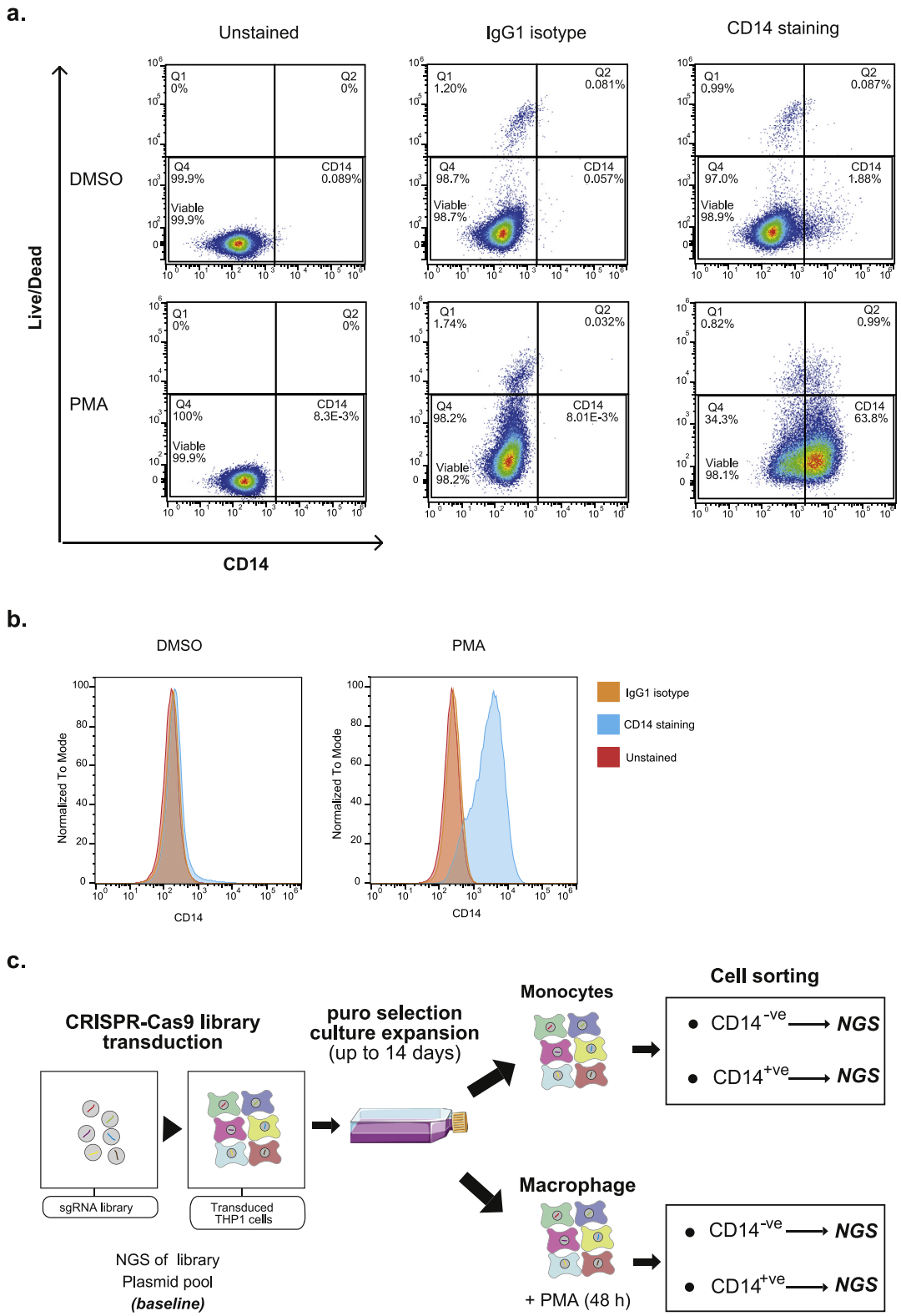

Fig. 1. THP-1 cells increase CD14 expression during macrophage differentiation. a. THP-1 cells increase the expression of CD14 after treatment for 48 h with the monocyte to macrophage differentiation factor PMA (100 ng/ml) in comparison to the DMSO control. b. Increased MFI values for CD14 expression after treatment with the differentiation factor PMA (100 ng/ml) for 48 h. c. Design of the CRISPR/Cas9 screen in THP-1 cells. A whole-genome library of guide RNAs was built in lentivirus plasmids with a selection marker (resistance to puromycin). THP-1 cells were transduced with lentivirus containing the plasmid, afterwards a culture selection in the presence of puromycin was performed. The remaining cells were treated for 48 h with 100 ng/ml of PMA to induce the differentiation into macrophages or DMSO (undifferentiated cells). Cell sorting was performed based on CD14 expression. The guide RNAs present in either the $CD14^{+ve}$ or $CD14^{-ve}$ cells from both groups were analysed. n = 3 biological replicates for each experiment.

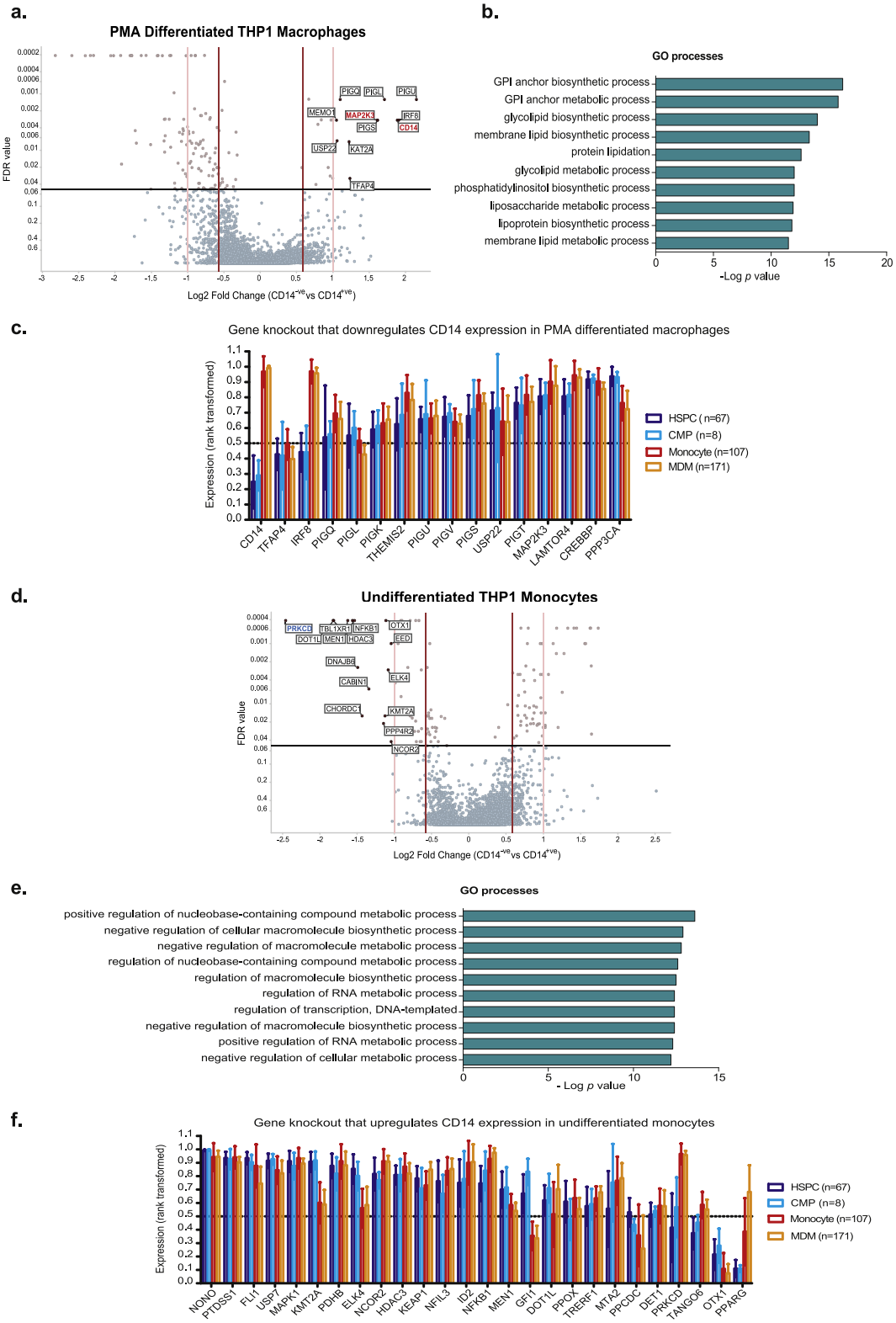

Fig. 2. Genes that modify CD14 expression in THP-1 cells. a. THP-1 monocytic cells transduced with a whole genome sgRNA library were differentiated into macrophages with 100 ng/ml of PMA for 48 h. Cells were sorted by flow cytometry based on CD14 expression. The volcano plots represent fold induction of sgRNAs of genes in the comparison of $CD14^{-ve}$ vs $CD14^{+ve}$ cells. A positive fold change means that the specific sgRNA is greater in $CD14^{-ve}$ cells which means that inhibition of that gene reduces the CD14 expression. Silencing of *CD14* and *MAP2K3* genes reduces the expression of CD14 in differentiated THP-1 cells. b. Top ten gene ontology processes by negative log *p* value in $CD14^{-ve}$ vs $CD14^{+ve}$ differentiated THP-1 monocytes, using positive Log2 fold change thresholds of 0.58 and a FDR *p* value threshold of 0.05. c. Stemformatics rank-transformed expression data for CRISPR screen hits within the myeloid lineage. Hematopoietic Stem and Progenitor Cells (HSPC, n = 67), Common Myeloid Progenitors (CMP, n = 8), peripheral blood monocytes

Stemformatics expression analysis

Median rank values (0 = no expression, 1 = highest expression) for each gene were assessed for primary cells collated in the Stemformatics myeloid atlas (28); Hematopoietic Stem and Progenitor Cells (HSPC, n = 67), Common Myeloid Progenitors (CMP, n = 8), peripheral blood monocytes (n = 171) and monocyte-derived macrophages (MDM, n = 107). Some genes lack an entry in the atlas compilation.

GO enrichment

A Log2-fold change threshold of 0.58 and FDR *p* value threshold of 0.05 was applied. The data was imported into MetaCore™ version 19.3 build 69800. Gene ontology (GO processes) enrichment was evaluated. The data for the top ten GO processes by Negative Log *p* value was exported for the figure. The GO processes table was generated from the genes listed in Supplementary Table 3 and 4.

Results

CD14 as a marker of activation during macrophage differentiation

THP-1 monocytic cells can be differentiated into macrophages using PMA (29). We tested a number of cell surface markers of activation and found that CD14 is one that was robustly increased after 48 h of treatment with 100 ng/ml of PMA (Fig. 1a). After treatment with PMA both the percentage of $CD14^{+ve}$ cells increased, as well as the mean fluorescence intensity (MFI) of CD14 expression per cell, as compared to the DMSO and isotype controls (Fig. 1a and 1b).

Based on these data and the fact that CD14 has been related to a pro-inflammatory phenotype in macrophages, we decided to use it as a readout during a CRISPR/Cas9 whole-genome screen to understand which genes are associated with the differentiation of inflammatory macrophages.

For screening, a library of sgRNAs targeting the whole genome with 6-fold redundancy were constructed in a plasmid containing a puromycin resistance cassette inserted into a lentivirus backbone (see materials and methods). THP-1 cells were transduced with the virus, expanded and selected in puromycin for 18 days (Fig. 1c). At this point, the cells were either differentiated into macrophages, by adding PMA for 48 h or kept as monocytes (DMSO vehicle control) for 48 h. After this differentiation step, the cells in each group were sorted by FACS based on CD14 expression and next-generation sequencing performed to identify the sgRNAs present in the individual populations.

Genes regulating CD14 expression

After sorting the cells based on CD14 expression, the sgRNAs present in the different populations were analysed. In PMA differentiated THP-1 macrophages the sgRNAs present in $CD14^{-ve}$ vs $CD14^{+ve}$ were analysed and represented in a volcano plot (Fig. 2a). A positive fold change in the volcano plots indicates that more sgRNA targeting a specific gene is present in the $CD14^{-ve}$ population than in the $CD14^{+ve}$. This means that the silencing of those genes reduces CD14 expression in THP-1 PMA differentiated macrophages. A list of the 21 significantly upregulated sgRNAs (L2FC > 0.58, FDR < 0.05) is presented as Supplementary Table 3. Crucially, one of the top hits is, of course, CD14 itself. As expected, there are also a number of genes that regulate phosphatidylinositol glycan (PIG) anchor biosynthesis, which would be required for CD14 adherence to the cell surface. Gene ontology analysis confirmed this observation, with the primary biological process implicated in biosynthetic processes underlying GPI anchors (Fig. 2b). Publicly available expression data from the Stemformatics platform reveals that the majority of these hits are highly ranked (top 50%) within the myeloid lineage, and that for some, the rank is increased after differentiation (Fig. 2c).

The same analysis was performed for undifferentiated THP-1 monocytes (Fig. 2d). In this case, we were interested in the sgRNAs with a negative fold change, which means they are enriched in $CD14^{+ve}$ cells, and thus these sgRNAs denote genes that when depleted result in spontaneous upregulation of CD14 expression. A list of the 36 significantly downregulated sgRNAs (L2FC < -0.58, FDR < 0.05) is presented as Supplementary Table 4. Gene ontology analysis showed significant enrichment of processes related to negative regulation of transcription, which is consistent with the deletion of these genes upregulating CD14 expression (Fig. 2e). Stemformatics expression data demonstrates that some of these negative regulators are downregulated during myeloid differentiation, but others are upregulated (Fig. 2f). Similar to the positive regulators in Supplementary Table 3, the majority of targets we have identified in Supplementary Table 4 are highly ranked (top 50%) within the myeloid lineage (Fig. 2f).

Screen validation by small molecule inhibition

As an alternative to conventional validation by repeating individual gene deletions using CRISPR, we searched available internal data and published resources for previously established on-target small molecule inhibitors of the screen hits. From this list we took the top 5 small molecules that target genes found in the screening of CD14 in either differentiated or undifferentiated THP-1 cells (Supplementary Table 1). All of these have literature references to support their on-target effect, with the exception of iPRKCD for which the profiling data is provided here (Supplementary Table 2).

For this validation assay, CD14 expression and sCD14 production were measured in THP-1 cells treated with the different inhibitors (at either 3 μM or 100 nM), in the absence (Fig. 3a) or presence of PMA (100 ng/ml) for 48 h (Fig. 3b). The different concentrations used for the compounds were based on studies of viability and MMP-9 expression (Supplementary Fig. 1). MMP-9 is produced by THP-1 as a result of differentiation with PMA (30). We identified one inhibitor that increased CD14 expression in the PMA differentiated cells (iPRKCD) and showed the same trend in undifferentated cells, although did not reach statistical significance (p = 0.06). Similar results were found for sCD14 with this compound, and again the trend in increase was not statistically different. We also identified two compounds that had a significant effect of decreasing CD14 expression in PMA differentiated macrophages (iMAP2K3 and iEIF2AK3). For differentiated cells iMAP2K3 also reduced the production of sCD14, and a similar trend was observed in undifferentiated cells. iPRKCD did not have an overall impact on cell viability but did lead to a small increase in the MFI of CD14 on undifferentiated THP-1 cells (Fig. 3c). iMAP2K3 actually led to a small increase in cell viability, but did not influence the MFI of CD14 expression on PMA differentiated THP-1 cells (Fig. 3d).

(n = 171) and monocyte-derived macrophages (MDM, n = 107). Some genes lack an entry in the atlas compilation. Mean ± SEM d. Transduced cells were left untreated for 48 h. Cells were sorted by flow cytometry based on CD14 expression. The fold induction of sgRNAs of genes in $CD14^{-ve}$ vs $CD14^{+ve}$ cells is presented in the volcano plots. The silencing of *PRKCD* increases the expression of CD14 in THP-1 undifferentiated cells. n = 3 biological replicates for the screen. e. Top ten gene ontology processes by negative log *p* value in $CD14^{-ve}$ vs $CD14^{+ve}$ undifferentiated THP-1 monocytes, using positive Log2 fold change thresholds of 0.58 and a FDR *p* value threshold of 0.05. f. Stemformatics rank-transformed expression data for CRISPR screen hits within the myeloid lineage. Hematopoietic Stem and Progenitor Cells (HSPC, n = 67), Common Myeloid Progenitors (CMP, n = 8), peripheral blood monocytes (n = 171) and monocyte-derived macrophages (MDM, n = 107). Some genes lack an entry in the atlas compilation. Mean ± SEM.

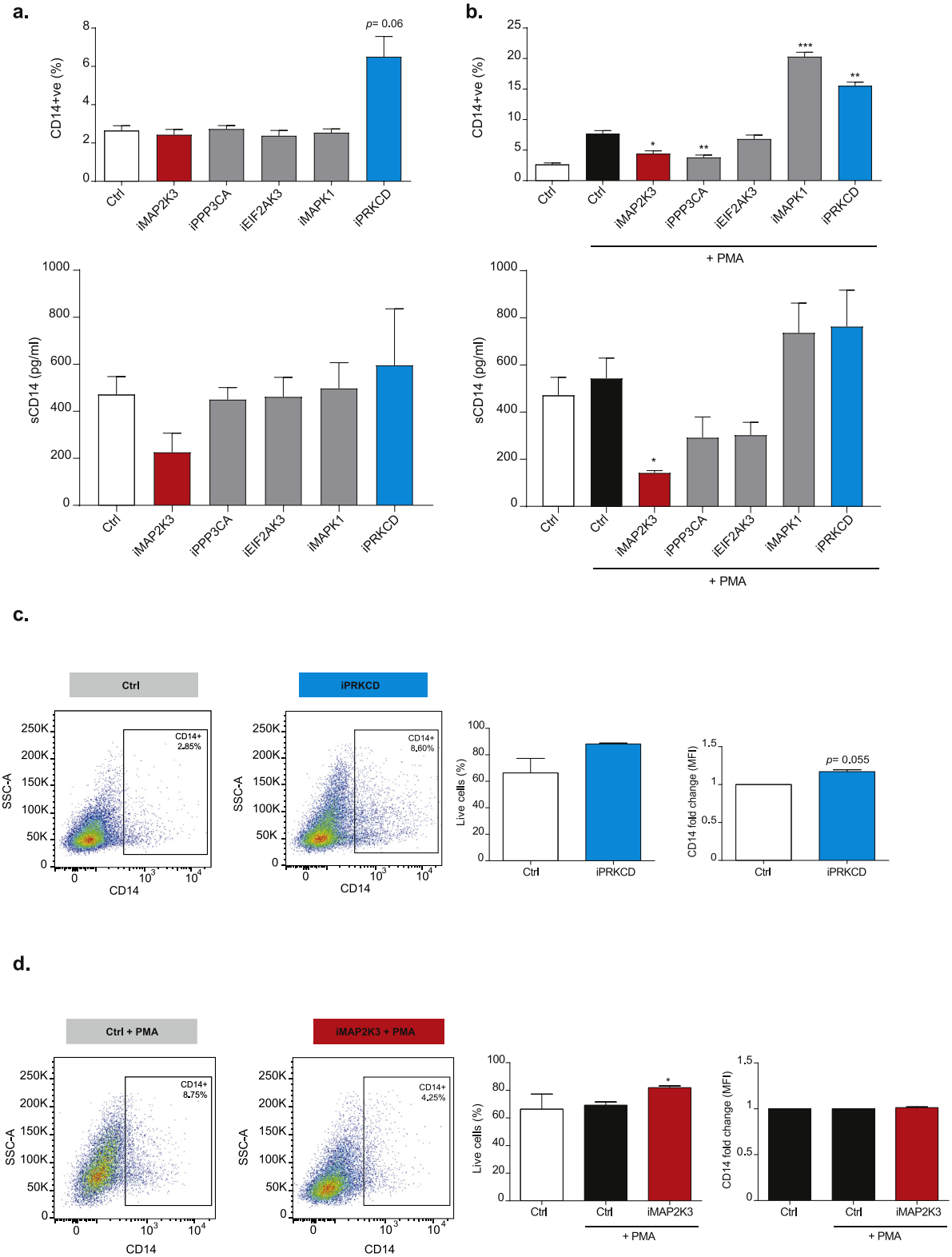

Fig. 3. small molecules to inhibit targets identified in the screen validate the results based on CD14 expression. a. THP-1 cells were left untreated for 48 h and were stimulated with either 3 μM or 100 nM of the different compounds. CD14^{+ve} cells were quantified by FACS and levels of sCD14 in the supernatant measured by ELISA b. THP-1 cells were differentiated into macrophages with PMA for 48 h (100 ng/ml) in combination with either 3 μM or 100 nM of the different compounds. CD14^{+ve} cells were quantified by FACS and levels of sCD14 in the supernatant measured by ELISA. c. Representative FACS analysis of THP-1 cells left untreated for 48 h in the presence of a PRKCD inhibitor (100 nM) and stained for CD14. The percentage of live cells and MFI fold change of CD14 normalized to DMSO (0.1%) control was then quantified. d. Representative FACS analysis of THP-1 cells treated with PMA (100 ng/ml) for 48 h in combination with a MAP2K3 inhibitor (100 nM) and stained for CD14. The percentage

Pharmacological modulation of CD14 in primary human macrophages

Although THP-1 are a human cell line, they are an immortalized monocytic leukaemia, and so we looked to translate our results to primary human macrophages, using *in vitro* differentiation of monocytes. Specifically, isolated human monocytes were cultured with M-CSF (100 ng/ml) and DMSO, 100 nM of iMAP2K3 or 100 nM of iPRKCD. After 5 days (Fig. 4a) we observed differences in the control macrophages compared to the treated macrophages. In the case of iMAP2K3 the macrophages lost the M-CSF elongated morphology and seem undifferentiated. iPRKCD treated MDMs retained the same morphology as the control macrophages.

Flow cytometry revealed that neither of the compounds significantly affected macrophage viability and that there was only a small reduction in the percentage of cells expressing CD14 for MDMs treated with iMAP2K3, which was not statistically significant (Fig. 4b). We also quantified CD16 expression, as an alternative readout of macrophage differentiation, and this was very significantly decreased by treatment with iMAP2K3 (Fig. 4b). The MFI of CD14 and CD16 expression in the macrophages was significantly decreased by iMAP2K3 but not iPRKCD (Fig. 4c).We also measured sCD14 production by these cells. We found a tendency to increase after the treatment with iPRKCD and decrease after iMAP2K3, although it did not reach statistical significance (Fig. 4d).

Finally, we wanted to study the effects of identified inhibitors on CD14 inflammatory signalling for the differentiated MDMs, when stimulated with LPS (100 ng/ml) for 24 h. As a readout, we measured the levels of pro-inflammatory cytokines (IL-1β, IL-6 and TNF). In agreement with the decreased expression of CD14 due to iMAP2K3, we observed a reduction in the production for all the cytokines tested in response to LPS (Fig. 4e). Although there was slightly increased cytokine production in iPRKCD differentiated cells treated with LPS, it did not reach statistical significance, which was also expected given that the expression of CD14 was not upregulated with this inhibitor.

Therefore, simply triaging known inhibitors of targets identified in a CRISPR screen of THP-1 differentiation has yielded at least one confirmed hit (MAP2K3) that translates through to effects on human primary pro-inflammatory macrophage function.

Discussion

In this work, we have used the human monocytic THP-1 cell line to model macrophage differentiation and CD14 upregulation after treatment with PMA. Immediately, it was possible to see that the screen was successful, with CD14 itself being one of the top hits (Fig. 2a). Moreover, many genes that were previously implicated in macrophage differentiation were also observed, providing further validation (Supplementary Table 3 and 4). However, this is not an exhaustive list of all pathways regulating macrophage differentiation and CD14, and certainly, PMA treated THP-1 cells are at best a model system. Therefore, we proceeded to validate hits from the screen with small molecules because these can be validated in primary human monocytes differentiated with M-CSF. As many of the novel targets for CD14 expression and macrophage differentiation from our primary screen do not have well-curated small molecule inhibitors established, they remain unvalidated at this point, and therefore this provides a novel resource to the community for future research. For example, the targets identified in Supplementary Table 4 could be useful in the context of cancer therapy, to terminally differentiate pro-myelocytic leukemic cell types like THP-1, which resulted from an MLL-AF9 translocation (31). Indeed, not only did we identify the gene encoding MLL (KMT2A) but also its upstream activator Id2 (32), and downstream targets DOT1L and MEN1 (33). Additionally, we suggest that a number of the novel targets identified could facilitate improved responses to infection or be utilised as adjuvants to vaccines.

From the list of selected inhibitors that we attempted to validate for the THP-1 differentiation process, only a few provided results that were in line with the initial genetic screen. This lack of translation could be due to a number of differences. In the genetic screening, many of the gene edits will remove the protein function entirely, however, with a small molecule inhibitor, some residual activity is likely. There could also be off-target effects of the compound, or the pharmacokinetics of inhibition may have been unfavourable in the assay. Additionally, we do not quantify cell death in real time, so the effects of phagocytosis may influence the end-point measurement. Of course, the initial hit from the screen may have been a false positive, so the small molecule inhibitor may not always be at fault.

After the validation in THP-1 cells, we tested if the molecules would show effects on primary MDM and found that only one compound had consistent results: iMAP2K3. Mitogen-activated protein kinase 3 (MAP2K3, MKK3) is a kinase that activates p38 MAPK in response to LPS (34) and a variety of other cell stressors such as cigarette smoke (35), Caerulin (36), TGF-β (37) and TNF (38). Therefore, this pathway regulates inflammatory pathology in models of sepsis (39), lung diseases (40–42), myocardial infarction (43) and diabetic nephropathy (44). Based on our data, either monocyte/macrophage differentiation or regulation of CD14 could account for the effects of MAP2K3 in these conditions, however, it may also have other roles in different cell types. The iMAP2K3 may be particularly effective at preventing inflammatory cytokine production from activated primary macrophages because we found it has a role during macrophage differentiation and CD14 downregulation and additionally it is known to regulate signalling downstream of CD14 (45,46). For these reasons, one could speculate that MAP2K3 inhibition may improve outcomes for patients suffering from COVID19, especially severe cases associated with inflammatory macrophages and sCD14 (47).

The other inhibitor that we progressed through to studies in primary MDMs was iPRKCD. PRKCD (Protein kinase delta) is a serine/threonine kinase that is activated downstream of diacylglycerol, and participates in a number of cell death/survival pathways (48). Based on the initial screens, iPRKCD should have had the effect to boost CD14 expression and downstream responses to LPS, however, despite a trend in that direction the differences were not statistically significant in differentiated primary MDMs. This was perhaps to be expected because PRKCD levels decrease significantly upon macrophage differentiation (49) and we observed the strongest effects when PRKCD was higher, in undifferentiated THP-1 monocytes (Fig. 3c). Overall, an effect of iPRKCD to promote macrophage differentiation and CD14 would be consistent with effects in mouse models of atherosclerosis where genetic deletion from macrophages decreased apoptosis, and increased macrophage number in aortic plaques (50). Whether beneficial effects of iPRKCD to fight infection or act as an adjuvant to vaccination could be harnessed without negative consequences is, therefore, a relevant issue.

In summary, we were able to identify genes that are important for the THP-1 macrophage differentiation process as a result of a CRISPR/Cas9 whole-genome screen. The screen identifies known pathways that validate the methodology, and novel hits that provide a new resource for the community. Based on these results, we were able to rapidly identify small molecules that would target select candidates and then translate our findings to primary human cells. In particular,

of live cells and MFI fold change of CD14 normalized to DMSO (0.1%) control was then quantified. Statistical significance was determined by unpaired *t*-test ($p < 0.05$). All error bars represent the SEM. n = 3 biological replicates for each experiment.

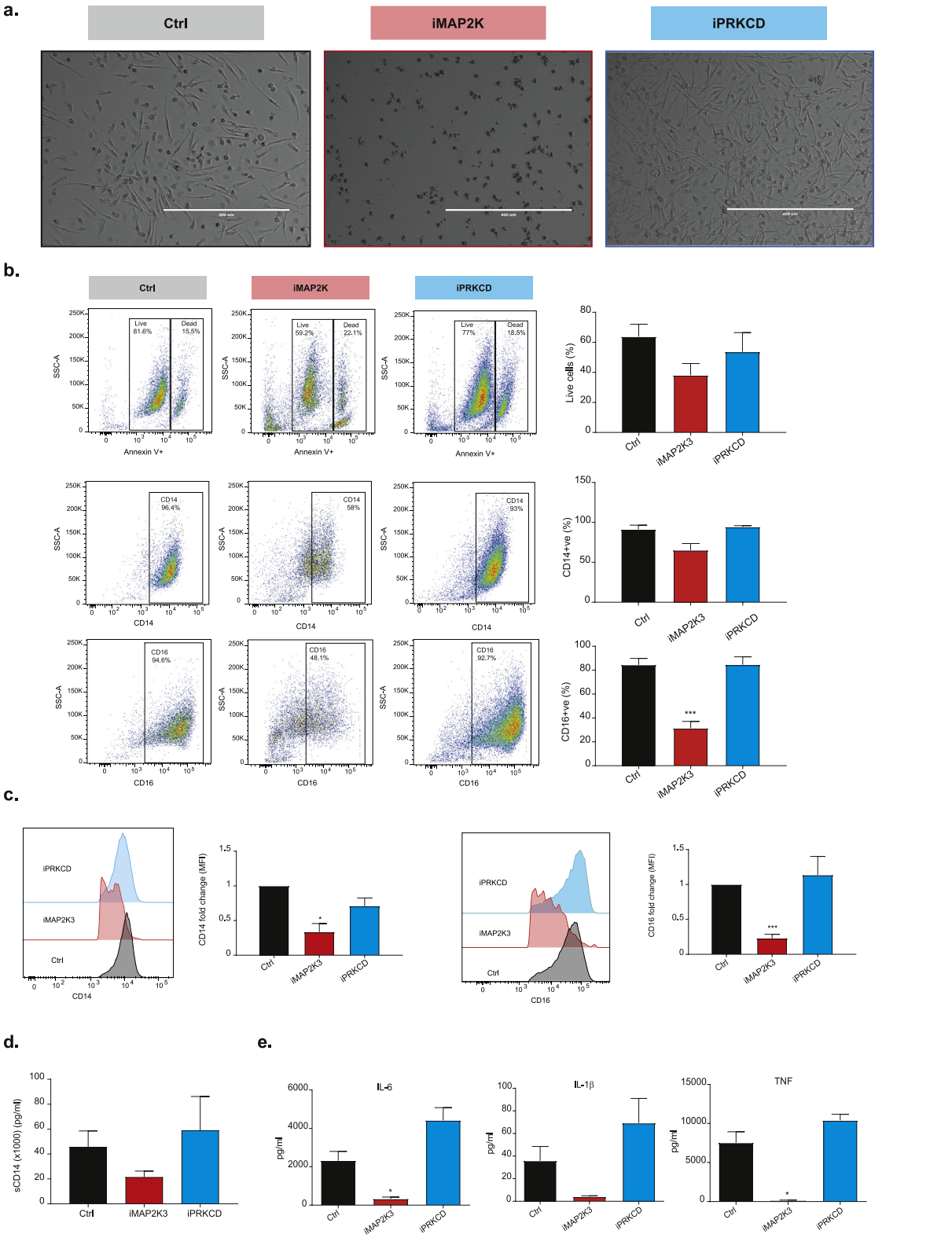

Fig. 4. Results from the THP-1 screen partially translate into human primary MCSF macrophages. Effect of the compounds on cytokine production. a. Morphology of human monocytes differentiated with M-CSF (100 ng/ml) into macrophages in the presence of an inhibitor for MAP2K3 (100 nM), PRKCD (100 nM) or DMSO control (0.1%). b. Percentage of live, CD14^{+ve} and CD16^{+ve} cells in the cells differentiated in the presence of the different compounds. c. MFI peaks and fold change values for CD14 and CD16 after treatment with both compounds and DMSO control. d. sCD14 production of MDM differentiated in the presence of MAP2K3 (100 nM), PRKCD (100 nM) or DMSO control (0.1%) was measured by ELISA e. Cells were differentiated in the presence of the two compounds, after differentiation cells were stimulated

iMAP2K3 showed the capacity to disrupt macrophage differentiation and CD14 dependent inflammation, and so represents a good candidate for testing in models of inflammatory disease, for example related to pathology due to COVID19.

Contributors

GJD, RLM, MP, CS, NB, CR and SB performed or assisted with experimentation. CAW provided bioinformatics support. GJD, RLM, MP, CS, EK, NB, CR, SB, RC, DA MPJdW, PKM and SLM were involved in experimental analysis and interpretation. All authors contributed to the writing and approved the final version of this manuscript.

Acknowledgments

This work was supported by a Viertel Senior Medical Research Foundation Fellowship (SLM) and the European Union's Horizon 2020 research and innovation program under Grant Agreement No. ITN-2014-EID-641665 [ITN-grant EPIMAC to MPJdW].

The CRISPR screens were conducted at Horizon Discovery (Cambridge, UK) and we would like to thank Benedict Cross for the replotting of Figures 1a and 1b for publication.

Authors who are GSK employee's had a role in paper design, data collection, data analysis, interpretation and writing of the paper.

Current affiliation for MP is Technology Transfer, LifeArc, Lynton House, 7-12 Tavistock Square, London, UK, WC1H 9LT, and for RC is Cinnabar Consulting Limited, Bedford, UK.

Declarations of interests

GJD, EK, SB, CS, NB, CR, NT, DA and PKM are employees and shareholders at GSK. MP and RC contributed to this manuscript whilst employees at GSK. SLM consults for IFM Therapeutics and received funding from GSK. MPJW reports grants from GSK outside the submitted work. The rest of the authors do not have anything to disclose regarding funding or conflicts of interest with respect to this manuscript.

Supplementary materials

Supplementary material associated with this article can be found, in the online version, at doi:10.1016/j.ebiom.2020.103039.

References

[1]] Wynn TA, Chawla A, Pollard JW. Macrophage biology in development, homeostasis and disease. Nature 2013;496(7446):445.
[2] Tabas I, Glass CK. Anti-inflammatory therapy in chronic disease: challenges and opportunities. Science 2013;339(6116):166–72.
[3] Landmann R, Müller B, Zimmerli W. CD14, new aspects of ligand and signal diversity. Microbes Infect 2000;2(3):295–304.
[4] Grage–Griebenow E, Flad HD, Ernst M. Heterogeneity of human peripheral blood monocyte subsets. J Leukoc Biol 2001;69(1):11–20.
[5] Gren ST, Rasmussen TB, Janciauskiene S, Håkansson K, Gerwien JG, Grip O. A single-cell gene-expression profile reveals inter-cellular heterogeneity within human monocyte subsets. PLoS One 2015;10(12):e0144351.
[6] Villani A-C, Satija R, Reynolds G, Sarkizova S, Shekhar K, Fletcher J, et al. Single-cell RNA-seq reveals new types of human blood dendritic cells, monocytes, and progenitors. Science 2017;356(6335) eaah4573.
[7] Cros J, Cagnard N, Woollard K, Patey N, Zhang S-Y, Senechal B, et al. Human CD14dim monocytes patrol and sense nucleic acids and viruses via TLR7 and TLR8 receptors. Immunity 2010;33(3):375–86.
[8] Tacke F, Alvarez D, Kaplan TJ, Jakubzick C, Spanbroek R, Llodra J, et al. Monocyte subsets differentially employ CCR2, CCR5, and CX3CR1 to accumulate within atherosclerotic plaques. J Clin Invest 2007;117(1):185–94.
[9] Auffray C, Fogg D, Garfa M, Elain G, Join-Lambert O, Kayal S, et al. Monitoring of blood vessels and tissues by a population of monocytes with patrolling behavior. Science 2007;317(5838):666–70.
[10] Ginhoux F, Jung S. Monocytes and macrophages: developmental pathways and tissue homeostasis. Nat Rev Immunol 2014;14(6):392–404.
[11] Ożańska A, Szymczak D, Rybka J. Pattern of human monocyte subpopulations in health and disease. Scand J Immunol. 2020:e12883.
[12] Antal–Szalmas P, Van Strijp JA, Weersink AJ, Verhoef J, Van Kessel KP. Quantitation of surface CD14 on human monocytes and neutrophils. J Leukoc Biol 1997;61(6):721–8.
[13] Wright SD, Ramos RA, Tobias PS, Ulevitch RJ, Mathison JC. CD14, a receptor for complexes of lipopolysaccharide (LPS) and LPS binding protein. Science 1990;249(4975):1431–3.
[14] Zanoni I, Ostuni R, Marek LR, Barresi S, Barbalat R, Barton GM, et al. CD14 controls the LPS-induced endocytosis of Toll-like receptor 4. Cell 2011;147(4):868–80.
[15] Labeta MO, Landmann R, Obrecht JP, Obrist R. Human B cells express membrane-bound and soluble forms of the CD 14 myeloid antigen. Mol Immunol 1991;28(1-2):115–22.
[16] Dunzendorfer S, Lee HK, Soldau K, Tobias PS. Toll–like receptor 4 functions intracellularly in human coronary artery endothelial cells: roles of LBP and sCD14 in mediating LPS–responses. FASEB J 2004;18(10):1117–9.
[17] Erridge C, Kennedy S, Spickett CM, Webb DJ. Oxidized phospholipid inhibition of toll-like receptor (TLR) signaling is restricted to TLR2 and TLR4 roles for cd14, lps-binding protein, and md2 as targets for specificity of inhibition. J Biol Chem 2008;283(36):24748–59.
[18] Pahwa R, Devaraj S, Jialal I. The effect of the accessory proteins, soluble CD14 and lipopolysaccharide-binding protein on Toll-like receptor 4 activity in human monocytes and adipocytes. Int J Obes 2016;40(6):907–11.
[19] Perera P-Y, Vogel SN, Detore GR, Haziot A, Goyert SM. CD14-dependent and CD14-independent signaling pathways in murine macrophages from normal and CD14 knockout mice stimulated with lipopolysaccharide or taxol. J Immunol 1997;158(9):4422–9.
[20] Ward TL, Goto K, Altosaar I. Ingested soluble CD14 contributes to the functional pool of circulating sCD14 in mice. Immunobiology 2014;219(7):537–46.
[21] Wu Z, Zhang Z, Lei Z, Lei P. CD14: Biology and role in the pathogenesis of disease. Cytokine Growth Factor Rev 2019;48:24–31.
[22] Martin TR, Wurfel MM, Zanoni I, Ulevitch R. Targeting innate immunity by blocking CD14: Novel approach to control inflammation and organ dysfunction in COVID-19 illness. E Bio Med 2020;57:102836.
[23] Messner CB, Demichev V, Wendisch D, Michalick L, White M, Freiwald A, et al. Ultra-high-throughput clinical proteomics reveals classifiers of COVID-19 infection. Cell Syst 2020.
[24] Martin TR, Rubenfeld GD, Ruzinski JT, Goodman RB, Steinberg KP, Leturcq DJ, et al. Relationship between soluble CD14, lipopolysaccharide binding protein, and the alveolar inflammatory response in patients with acute respiratory distress syndrome. Am J Respir Crit Care Med 1997;155(3):937–44.
[25] Sanjana NE, Shalem O, Zhang F. Improved vectors and genome-wide libraries for CRISPR screening. Nat Methods 2014;11(8):783.
[26] Cross BC, Lawo S, Archer CR, Hunt JR, Yarker JL, Riccombeni A, et al. Increasing the performance of pooled CRISPR–Cas9 drop-out screening. Sci Rep 2016;6(1):1–8.
[27] Li W, Xu H, Xiao T, Cong L, Love MI, Zhang F, et al. MAGeCK enables robust identification of essential genes from genome-scale CRISPR/Cas9 knockout screens. Genome Biol 2014;15(12):554.
[28] Rajab N, Angel P, Deng Y, Gu J, Jameson V, Kurowska-Stolarska M, et al. iMAC: an interactive atlas to explore phenotypic differences between in vivo, ex vivo and in vitro-derived myeloid cells in the Stemformatics platform. bioRxiv. 2020:719237.
[29] Daigneault M, Preston JA, Marriott HM, Whyte MK, Dockrell DH. The identification of markers of macrophage differentiation in PMA-stimulated THP-1 cells and monocyte-derived macrophages. PLoS One 2010;5(1):e8668.
[30] Zhou J, Zhu P, Jiang JL, Zhang Q, Wu ZB, Yao XY, et al. Involvement of CD147 in overexpression of MMP-2 and MMP-9 and enhancement of invasive potential of PMA-differentiated THP-1. BMC Cell Biol 2005;6(1):1–10.
[31] Odero MD, Zeleznik–Le NJ, Chinwalla V, Rowley JD. Cytogenetic and molecular analysis of the acute monocytic leukemia cell line THP–1 with an MLL–AF9 translocation. Genes Chromosom Cancer 2000;29(4):333–8.
[32] Ghisi M, Kats L, Masson F, Li J, Kratina T, Vidacs E, et al. Id2 and E proteins orchestrate the initiation and maintenance of MLL-rearranged acute myeloid leukemia. Cancer Cell 2016;30(1):59–74.
[33] Marschalek R. MLL leukemia and future treatment strategies. Arch Pharm (Weinheim) 2015;348(4):221–8.
[34] Ronkina N, Kotlyarov A, Dittrich-Breiholz O, Kracht M, Hitti E, Milarski K, et al. The mitogen-activated protein kinase (MAPK)-activated protein kinases MK2 and MK3 cooperate in stimulation of tumor necrosis factor biosynthesis and stabilization of p38 MAPK. Mol Cell Biol 2007;27(1):170–81.
[35] Mannam P, Rauniyar N, Lam TT, Luo R, Lee PJ, Srivastava A. MKK3 influences mitophagy and is involved in cigarette smoke-induced inflammation. Free Radic Biol Med 2016;101:102–15.
[36] Jia R, Ma J, Xiang S, Meng W, Wang N. Caerulin-induced pro-inflammatory response in macrophages requires TRAF3-p38 signaling activation. Biochem Biophys Res Commun 2017;494(1-2):358–64.

with LPS (100 ng/ml) for 24 h and IL-1β, IL-6, TNF levels were measured. Statistical significance was determined by unpaired t-test ($p < 0.05$). All error bars represent the SEM. n = 4 biological replicates for flowcytometry experiments and n = 3 biological replicates for the stimulation and ELISA experiments.

[37] Kim SI, Kwak JH, Zachariah M, He Y, Wang L, Choi ME. TGF-β-activated kinase 1 and TAK1-binding protein 1 cooperate to mediate TGF-β1-induced MKK3-p38 MAPK activation and stimulation of type I collagen. Am J Physiol-Renal Physiol 2007;292(5):F1471–F8.
[38] Inoue T, Boyle DL, Corr M, Hammaker D, Davis RJ, Flavell RA, et al. Mitogen-activated protein kinase kinase 3 is a pivotal pathway regulating p38 activation in inflammatory arthritis. Proc Natl Acad Sci 2006;103(14):5484–9.
[39] Mannam P, Shinn AS, Srivastava A, Neamu RF, Walker WE, Bohanon M, et al. MKK3 regulates mitochondrial biogenesis and mitophagy in sepsis-induced lung injury. Am J Physiol-Lung Cell Mol Physiol 2014;306(7):L604–L19.
[40] Holand T, Riffo-Vasquez Y, Spina D, O'Connor B, Woisin F, Sand C, et al. A role for mitogen kinase kinase 3 in pulmonary inflammation validated from a proteomic approach. Pulm Pharmacol Ther 2014;27(2):156–63.
[41] Otterbein LE, Otterbein SL, Ifedigbo E, Liu F, Morse DE, Fearns C, et al. MKK3 mitogen-activated protein kinase pathway mediates carbon monoxide-induced protection against oxidant-induced lung injury. Am J Pathol 2003;163(6):2555–63.
[42] Mannam P, Zhang X, Shan P, Zhang Y, Shinn AS, Zhang Y, et al. Endothelial MKK3 is a critical mediator of lethal murine endotoxemia and acute lung injury. J Immunol 2013;190(3):1264–75.
[43] Du J, Zhang L, Wang Z, Yano N, Zhao YT, Wei L, et al. Exendin-4 induces myocardial protection through MKK3 and Akt-1 in infarcted hearts. Am J Physiol-Cell Physiol 2016;310(4):C270–C83.
[44] Lim AKH, Nikolic-Paterson DJ, Ma F, Ozols E, Thomas MC, Flavell RA, et al. Role of MKK3−p38 MAPK signalling in the development of type 2 diabetes and renal injury in obese db/db mice. Diabetologia 2009;52(2):347–58.
[45] Nick JA, Avdi NJ, Young SK, Lehman LA, McDonald PP, Frasch SC, et al. Selective activation and functional significance of p38α mitogen-activated protein kinase in lipopolysaccharide-stimulated neutrophils. J Clin Invest 1999;103(6):851–8.
[46] Srivastava A, Shinn AS, Lee PJ, Mannam P. MKK3 mediates inflammatory response through modulation of mitochondrial function. Free Radic Biol Med 2015;83:139–48.
[47] Wang C, Xie J, Zhao L, Fei X, Zhang H, Tan Y, et al. Alveolar macrophage dysfunction and cytokine storm in the pathogenesis of two severe COVID-19 patients. E Bio Med 2020;57:102833.
[48] Malavez Y, Gonzalez-Mejia ME, Doseff AI. PRKCD (protein kinase C, delta). Atlas Genet Cytogenet Oncol Haematol 2009.
[49] Yamada K, Sakane F, S-i Imai, Tsushima S, Murakami T, Kanoh H. Regulatory role of diacylglycerol kinase γ in macrophage differentiation of leukemia cells. Biochem Biophys Res Commun 2003;305(1):101–7.
[50] Li Q, Park K, Xia Y, Matsumoto M, Qi W, Fu J, et al. Regulation of macrophage apoptosis and atherosclerosis by lipid-induced PKCδ isoform activation. Circ Res 2017;121(10):1153–67.